



Article

Study of the Adsorption of *Bacillus subtilis* and *Bacillus cereus* Bacteria on Enterosorbent Obtained from Apricot Kernels

Lucian Lupascu, Oleg Petuhov, Nina Timbaliuc  and Tudor Lupascu *

Institute of Chemistry, Str. Academiei, Nr. 3, MD-2028 Chisinau, Moldova; lucianlupascu75@gmail.com (L.L.); petuhov.chem@gmail.com (O.P.); timbaliuc_nina@yahoo.com (N.T.)

* Correspondence: lupascut@gmail.com

Abstract: This paper presents the results of scientific research on the structural parameters and the adsorption capacity of activated carbon obtained from apricot kernels (AC-A) in a fluidized layer. The obtained results highlight the fact that the described procedure allows obtaining a mesoporous carbon adsorbent with increased adsorption capacities ($S_{\text{BET}} = 1424 \text{ m}^2/\text{g}$) and with quality indices corresponding to the requirements of the carbon enterosorbents imposed by the European Pharmacopoeia Monograph. Adsorption kinetics studies of the bacteria *Bacillus subtilis* and *Bacillus cereus* have shown that the time to establish the adsorption equilibrium is 75–90 min. The adsorption of the mentioned bacteria on the carbon enterosorbent AC-A was studied depending on the temperature (26 and 36 °C) and pH of the solution (1.97–4.05). Scanning Electron Microscopy (SEM) showed that the immobilization of bacteria takes place on the outer surface of the carbon adsorbent due to the fact that the geometric dimensions of the bacteria are often larger than the macro diameter of the activated carbon pores. FTIR investigations also indicated the presence of bacteria on the surface of the activated carbon.

Keywords: *Bacillus subtilis*; *Bacillus cereus*; activated carbon; adsorption; SEM; FTIR



Citation: Lupascu, L.; Petuhov, O.; Timbaliuc, N.; Lupascu, T. Study of the Adsorption of *Bacillus subtilis* and *Bacillus cereus* Bacteria on Enterosorbent Obtained from Apricot Kernels. *C* **2022**, *8*, 38. <https://doi.org/10.3390/c8030038>

Academic Editor: Joaquín Silvestre-Albero

Received: 20 June 2022

Accepted: 6 July 2022

Published: 8 July 2022

Publisher's Note: MDPI stays neutral with regard to jurisdictional claims in published maps and institutional affiliations.



Copyright: © 2022 by the authors. Licensee MDPI, Basel, Switzerland. This article is an open access article distributed under the terms and conditions of the Creative Commons Attribution (CC BY) license (<https://creativecommons.org/licenses/by/4.0/>).

1. Introduction

One of the main problems of modern medicine of this century is intoxication of human organisms as a result of the negative state of the environment. Enterosorption is one of the safest and most effective methods for removing toxic substances, based on oral administration of drugs that can absorb various toxic substances of endogenous and exogenous origin in the lumen of the gastrointestinal tract without entering into chemical reactions with them [1]. Enterosorbents are widely used to treat diseases of the human body caused by pathogenic bacteria and to detoxify it in the case of poisoning with various chemicals [2]. Enterosorbents are a group of materials that include activated carbon, clay minerals, polymeric resins, and silicates [3–5]. The human intestinal microbiota are a complex ecosystem formed by gut microbes, which co-evolve and interact with their host [6]. Imbalance, dysfunction, or disturbance of the gut microbiota are increasingly recognized as indicators of a given disease or a poor health status [7]. Bacteria are vital organisms in many ecological cycles, having the role of circulating nutrients, as is the case of nitrogen fixation in the Earth's atmosphere. Another example is the decomposition of corpses, the bacteria being responsible for the putrefaction stages of this process. There are many pathogenic species among bacteria, which cause infectious diseases in humans, animals, and plants. Many species of bacteria are used in the food industry, in the mining industry, in the cleaning of wastewater, in the production of bacterial fertilizers, and in some medicinal preparations [8–11].

A large number of bacteria is found in the intestinal flora and a large percentage of them are represented by the skin microflora. The vast majority of bacterial species that live in the human body are considered harmless due to the body's specific defense mechanisms,

such as the immune system. There are also bacteria that are beneficial, especially those belonging to the intestinal flora. Despite this, some species are pathogenic and, once entering the body, cause various infectious diseases, including cholera, anthrax, leprosy, bubonic plague, and pneumonia. The most common fatal bacterial infectious diseases are respiratory infections, tuberculosis killing about 2 million people each year, mostly in sub-Saharan Africa [12–17].

The influence of the growth phase of *Pseudomonas putida* on its adhesion to kaolinite-coated slides was studied in the paper [18]. Steady-phase cells have been shown to have a higher adsorption density on kaolinite surfaces than mid-exponential phase cells under static deposition conditions. Compared to mid-exponential phase cells, stationary phase cells had a higher saturation coverage. The higher adhesion of the cells in the stationary phase was probably due to their smaller size and lesser negative surface loads compared to the cells of other growth stages, which led to deeper secondary energy minimums and lower energy barriers for adhesion. The results of this study suggest that the growth phase may strongly influence cell mobility and biofilm formation in aqueous geochemical environments.

The influence of temperature, pH, and salt concentration on the adsorption of *Bacillus subtilis* bacteria on the minerals kaolinite, montmorillonite, and goethite was studied in the paper [19].

Article [20] presents the results of scientific research aimed at immobilizing pathogenic bacteria on silicon dioxide and aluminosilicates obtained from rice husk and straw. It has been established that the adsorption of the bacteria *Escherichia coli*, *Bacillus subtilis*, *Pseudomonas aeruginosa*, and *Staphylococcus aureus* from natural waters is more pronounced compared to the value of immobilization of these bacteria on similar adsorbents obtained by traditional technologies.

Granular activated carbons must be used for the removal of toxic organic substances as well as pathogenic microorganisms from the natural waters in their drinking water technologies. The analysis of the scientific results obtained demonstrates that the use of activated carbon in technological processes allows to obtain a drinking water that corresponds to the norms of quality [21]. The paper [22] presents the results of scientific research aimed at the use of carbon enterosorbents impregnated with antibiotics in the process of reducing the increased growth of pathogenic bacteria in the human body. The use of sulfamethoxazole-impregnated carbon enterosorbents has been shown to reduce the growth of *S. aureus* and *E. coli* bacteria by 47–72%, and gentamicin-impregnated ones obstruct the growth of the bacteria by 50%. The results obtained offer a new opportunity for the use of carbon adsorbents in the processes of pronounced elimination of pathogens from the human body.

The interaction between carbon nanotubes (CNTs) and microorganisms: the antimicrobial effects of single-walled, multi-walled, functionalized, and non-functionalized CNTs; the mechanism of action of these nanomaterials at the unicellular level; and their effects on soil and aquatic microorganisms were studied in the paper [23]. Among the mechanisms of action of CNTs on the microbial cell are direct contact, which leads to the destruction of the cell wall and cytoplasmic membrane, changes in membrane fluidity, oxidative stress, enzyme inhibition, and reduced transcription of several key genes. It has been shown that the antimicrobial effect of CNTs strongly depends on the diameter, length, degree of aggregation, concentration, surface functionalization, degree of purification, time, and intensity of contact [23].

Another area of interest in the study of the adsorption of microorganisms on adsorbents is bioremediation. Bioremediation using different microorganisms, including bacteria, fungi, microalgae, and yeast, provides an eco-friendly and cost-effective alternative to traditional physical or/and chemical remediation methods; previous studies have reported that a multitude of microorganisms have high heavy metals tolerance and biosorption capacity [24,25].

The two species used in the study are representatives of the group of Gram-positive bacteria, such as *Bacillus subtilis* and *Bacillus cereus*. These bacteria were isolated from soil samples and grown on nutrient agar for the accumulation of bacterial biomass. They occur naturally in soils, at a concentration of up to one million per gram, and are therefore some of the most common bacteria that can be grown in the soil. Moreover, because of the structure similarity with bacteria from other groups, these species can be used as test-models for the evaluation of the adsorptive properties of the activated carbon for bacteria from different species.

The analysis of the bibliographic sources in the field of adsorption of bacteria on different solid supports allows us to conclude that this technology, with the involvement of intact carbon adsorbents, is not attested. The aim of our studies was to investigate the adsorption processes of some bacteria on intact activated charcoal obtained from apricot kernels.

2. Materials and Methods

2.1. Bacteria

The study used 2 species of bacteria, representatives of the groups of Gram-positive bacteria such as: *Bacillus subtilis*, *Bacillus cereus*. The bacterial species *Bacillus subtilis* and *Bacillus cereus* were isolated from soil samples and grown on nutrient agar for the accumulation of bacterial biomass.

In order to carry out research for bacterial adsorption on activated carbon, solutions of these bacteria with an optical density of 0.48 were prepared, in a tub with the length of 10 mm recorded on the КФК-2-УХЛ photo colorimeter 4.2, or 1.9 according to the McFarland index, determined by the DEN-1 densimeter (BIOSAN). Amounts of 5, 10, 15, . . . , and 50 mL of prepared bacterial solution were placed in 10 vials, to which 45, 40, 35, . . . , 5 mL of distilled water was added, respectively, to dilute the initial prepared solutions. Subsequently, calibration curves were established for each bacterial species studied. The prepared solutions were then contacted with pre-weighed activated carbon samples to the nearest 0.0001 (approx. 100 mg each). After 120 min of contact, the optical densities of the studied samples were measured at a wavelength of 315 nm, and subsequently the equilibrium concentrations and the adsorption values were calculated.

2.2. Obtaining Activated Carbon

Activated carbon (AC-A) was obtained from apricot kernels in a fluidized layer at a temperature of 1000 °C by activation with steam for 30 min. Water consumption throughout activation was 130 mL. The sample were dried at 110 °C, sieved to 90 < fraction < 125 µm size, and stored for analysis.

2.3. Gas Adsorption

Structure and adsorption parameters of samples were obtained from nitrogen adsorption-desorption isotherms at 77 K. The adsorption isotherms were measured using Autosorb-1-MP (Quantachrome, Boynton Beach, Florida, United States), with prior degassing at 60 °C for 12 h. The specific surface area (SBET) was calculated using the Brunauer-Emmett-Teller (BET) equation. The total pore volume (V_s) was calculated by converting the amount of adsorbed N_2 gas at a relative pressure of 0.99 to equivalent liquid volume of the adsorbate (N_2). The micropore volume (V_{mi}) was determined using t-method, the pore volume distribution curve was established using the DFT method. The quality indices of the enterosorbent AC-A were established according to the methodology of the European Pharmacological Monograph, edition 10 [26].

2.4. Determination of the Kinetics of the Adsorption Process of Bacteria on Carbon Enterosorbents

Amounts of 200 mg of activated carbon and 200 mL of bacterial solution with the initially established concentration were placed in a 300 mL glass flask. The balloon was fixed in an electric stirrer and stirring was started at a frequency of 150 rpm. After every

15 min of stirring, 2 mL of solution was taken and the equilibrium concentration was determined, along with the value of adsorption. The solution in the vat was returned to keep the volume of the solution constant. The time in which the equilibrium of the adsorption process was established experimentally from the graph of the dependence of the adsorption value on the agitation time.

2.5. Adsorption Study

Adsorption isotherms of bacteria were measured at different temperatures after stirring the bacterial solutions of different initial concentrations with carbon adsorbents for 2 h. For this, 100 mg of adsorbent were passed into flasks of 150 mL. A 50 mL solution of bacteria of different initial concentrations was passed into each flask. The flasks were fixed in a mechanical stirrer with a water thermostat and allowed to stir for 2 h at 150 rot/min. The adsorption capacity values for the bacteria were determined by the expression: $a = (C_0 - C_e) \times V/m$ (1) where: a —represents the adsorption capacity of the adsorbent ($\text{McF} \times 10^8/\text{g}$); C_0 represents the initial concentration of the adsorbate ($\text{McF} \times 10^8/\text{L}$); C_e is the equilibrium concentration of the adsorbate ($\text{McF} \times 10^8/\text{L}$); V is the volume of the contact solution (L); m is the mass of the adsorbent (g). To model the pH in the stomach, adsorption at pH 1.97 was performed using a sodium citrate-hydrochloric acid buffer solution as a solvent.

Langmuir isotherm model is an empirical model assuming that adsorption can only occur at a finite number of definite localized sites, and the adsorbed layer is one molecule in thickness or monolayer adsorption. The non-linear expression of the Langmuir isotherm model can be illustrated as Equation (1)

$$q_e = \frac{q_m K_L C_e}{1 + K_L C_e} \quad (1)$$

where C_e is the concentration of solution at equilibrium ($\text{McF} \times 10^8/\text{L}$); q_e is the corresponding adsorption capacity ($\text{McF} \times 10^8/\text{g}$); and q_m ($\text{McF} \times 10^8/\text{g}$) and K_L ($\text{L}/\text{McF} \times 10^8$) are constants which are related to adsorption capacity and energy or net enthalpy of adsorption, respectively.

The Freundlich isotherm model is the relationship describing the non-ideal and reversible adsorption, which can be applied to multilayer adsorption, on the basis of an assumption concerning the energetic surface heterogeneity. The non-linear expression of Freundlich isotherm model can be illustrated as Equation (2):

$$q_e = K_F C_e^{1/n} \quad (2)$$

where constant, K_F measures the relative adsorption capacity of the adsorbent and the slope $1/n$, ranging between 0 and 1, is a measure for the adsorption affinity or surface heterogeneity.

The linear forms of the Langmuir and Freundlich isotherms models are given in Equations (3) and (4), respectively:

$$\frac{C_e}{q_e} = \frac{1}{q_m K_L} + \frac{C_e}{q_m} \quad (3)$$

$$\ln q_e = \ln K_F + 1/n \ln C_e \quad (4)$$

Hence by plotting C_e/q_e against C_e it is possible to obtain the value of the Langmuir constants K_L and q_m and by plotting $\ln(q_e)$ against $\ln(C_e)$, the Freundlich constants of K_F and n can be determined.

2.6. Scanning Electron Microscopy

Scanning electron microscopy (SEM) images were obtained on JSM-6060 equipment. This is a high-resolution analytical SEM that can reach 2.5 nm resolution at an accelerating voltage of 30 kV. The electron source is a tungsten hairpin gun.

2.7. Fourier Transform Infrared Spectra

Measurements by Fourier transform infrared (FTIR) spectra were registered with an infrared Fourier transform spectrophotometer (Thermo Nicolet, NEXUS 670, USA). For this purpose, the samples were ground in an agate mortar and pressed with KBr.

3. Results and Discussion

The nitrogen adsorption–desorption isotherm on AC-A activated carbon is shown in Figure 1a. The structural parameters of the adsorbent, Table 1, indicate that AC-A is a mixed pore adsorbent, predominantly mesoporous. The same results can be seen from the pore volume distribution curve as a function of diameter, Figure 1b.

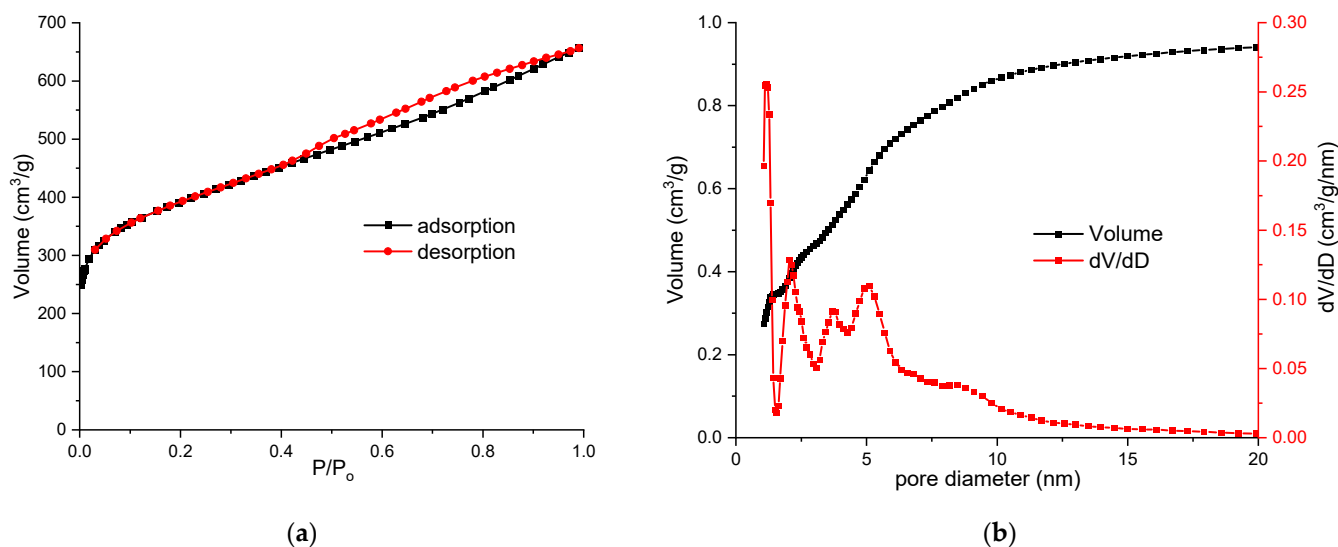


Figure 1. Nitrogen adsorption–desorption isotherms (a) and pore volume distribution curves (b) for sample AC-A.

Table 1. Structural parameters and specific surface area of the AC-A enterosorbent.

Sample	S_{BET} , m^2/g	V_s , cm^3/g	V_{mi} , cm^3/g	V_{me} , cm^3/g
AC-A	1424	1.016	0.332	0.684

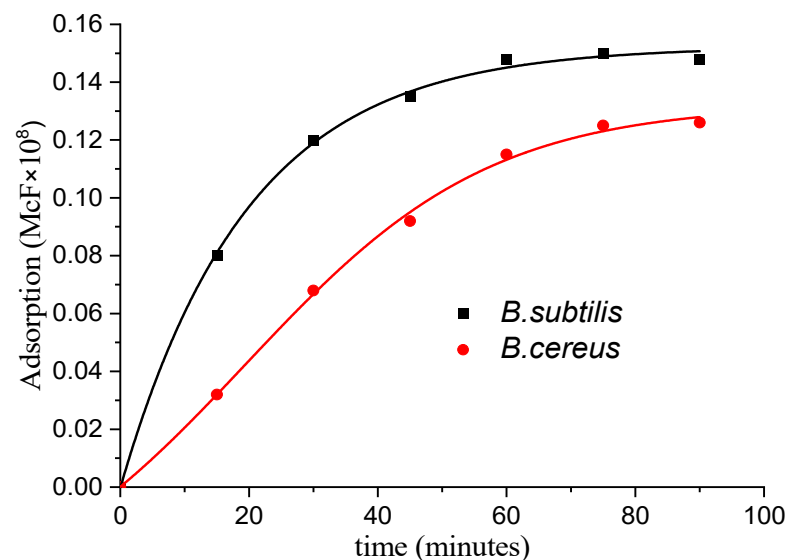
Structural parameters and specific surface area of the AC-A enterosorbent are shown in Table 1. The analysis of the data presented in Table 1 allows us to conclude that by applying the method of obtaining activated carbon in a fluidized layer we obtain mesoporous carbon adsorbents with specific pronounced surfaces.

The quality indices of the AC-A enterosorbent determined in accordance with the methodology set out in the European Pharmacopoeia Monograph, edition 10, are presented in Table 2. The analysis of the data presented in Table 2 allows us to conclude that the quality indices of activated carbon AC-A correspond to the quality standards required by the European Pharmaceutical Monograph, 10th edition imposed for carbon enterosorbents.

The kinetics of the adsorption processes of *Bacillus subtilis* and *Bacillus cereus* bacteria is shown in Figure 2.

Table 2. Quality indices of the AC-A enterosorbent.

Quality Indices	The Set Value	Allowable Value
Loss of mass on drying	1.62%	maximum 15%
Ash after US STAS	3.44%	maximum 5%
Acid-soluble substances	2.73%	maximum 3%
Copper content	<3.58 ppm	maximum 25 ppm
Lead content	<1.25 ppm	maximum 10 ppm
Zinc content	19.81 ppm	maximum 25 ppm
Adsorption power	40.7 g phenazone at 100 AC	minimum 40.0 g phenazone at 100 AC

**Figure 2.** Adsorption kinetics of *B. subtilis* and *B. cereus* bacteria on activated carbon AC-C.

The analysis of the results presented in Figure 2 allows us to conclude that the equilibrium of the adsorption process of *B. subtilis* bacteria is established after 75 min of stirring, and in the case of *B. cereus* bacteria the equilibrium is established in 90 min.

The adsorption isotherms of *B. subtilis* and *B. cereus* bacteria measured after 120 min of stirring at a frequency of 150 rpm at different pH values and at different temperatures are shown in Figures 3 and 4.

The analysis of the adsorption isotherms of the bacteria presented in Figures 3 and 4 allow us to conclude that the adsorption process of the bacteria is an exothermic one, i.e., with the increase in the temperature, the adsorption value decreases. The pH value of the solution has a different influence. In the case of *B. subtilis*, the decrease in pH leads to an increase in the amount of immobilized bacteria per unit area of carbon adsorbent, and in the case of *B. cereus* bacteria the effect is the opposite, a decrease in pH leads to a decrease in the number of immobilized bacteria on the carbon enterosorbent.

In Table 3 are presented the constants and correlation coefficients calculated by means of Langmuir and Freundlich equations; one may note that the Langmuir model describes better the adsorption of *B. subtilis* and *B. cereus*. This may be explained through the localized adsorption on active centers, which are the functional groups of activated carbon. The value of the Langmuir constant, K_L , decreases with the increase the temperature which denotes the exothermic effect of the immobilization process.

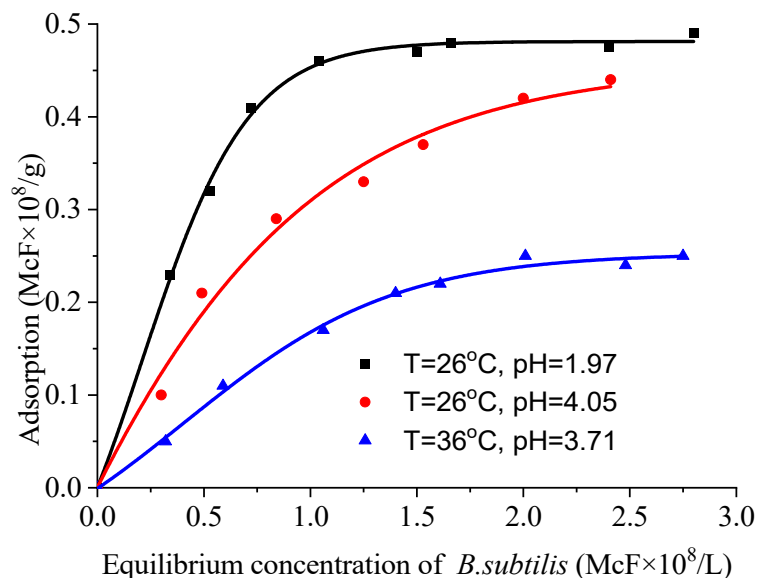


Figure 3. Adsorption isotherm of *B. subtilis* bacterium on AC-A enterosorbent.

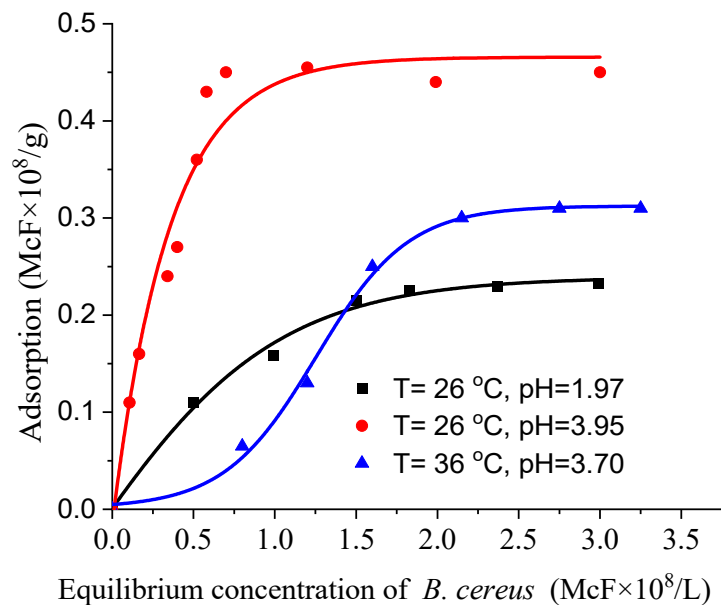


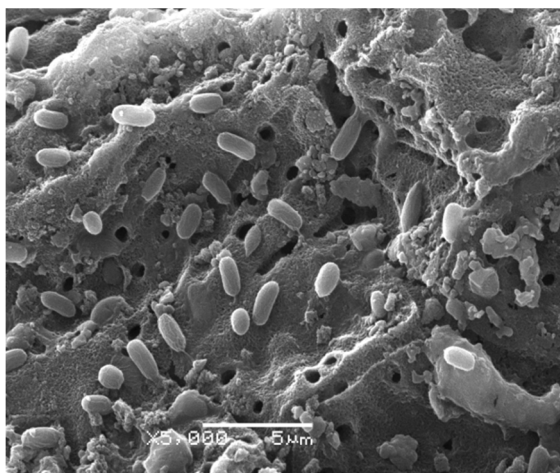
Figure 4. Adsorption isotherm of *Bacillus cereus* bacterium on AC-A enterosorbent.

Table 3. Langmuir and Freundlich isotherm constants and correlation coefficients of *B. subtilis* and *B. cereus* adsorption capacity on AC-A.

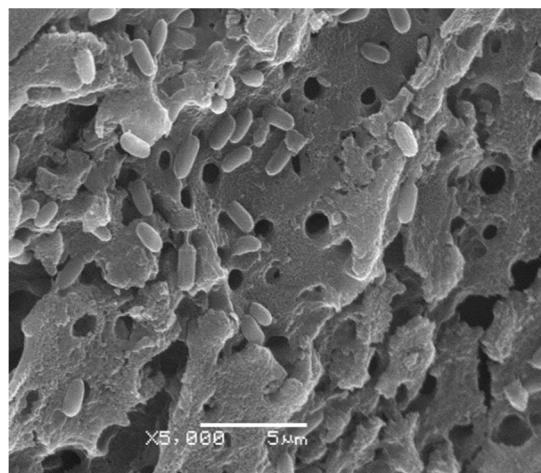
Bacteria	T, °C	pH	q_m^* , McF × 10 ⁸ /g	Langmuir			Freundlich		
				q_m , McF × 10 ⁸ /g	K_L , L/McF × 10 ⁸	R ²	K_F	n	R ²
<i>B. subtilis</i>	26	1.97	0.475	0.534	3.552	0.991	0.387	3.48	0.759
	26	4.05	0.450	0.607	1.052	0.996	0.300	2.28	0.983
	36	3.71	0.260	0.356	0.902	0.972	0.141	1.47	0.910
<i>B. cereus</i>	26	1.97	0.233	0.307	1.236	0.978	0.160	2.24	0.920
	26	3.95	0.455	0.502	3.877	0.983	0.586	1.33	0.984
	36	3.70	0.310	0.398	1.188	0.974	0.105	0.88	0.871

*—experimental adsorption capacity.

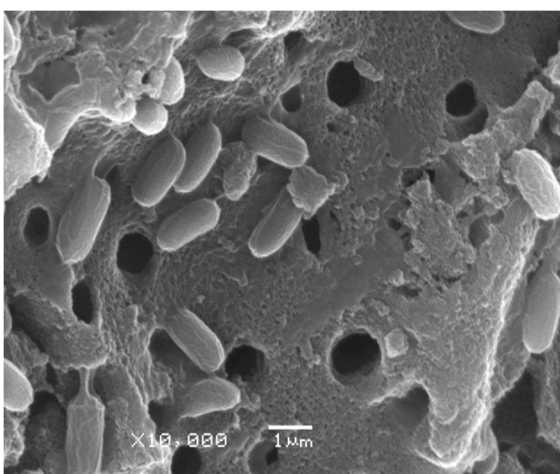
Scanning electron microscopy of the bacteria *Bacillus subtilis* and *Bacillus cereus* adsorbed on the AC enterosorbent at a scale of 1: 5000 and 1: 10,000 are shown in Figure 5.



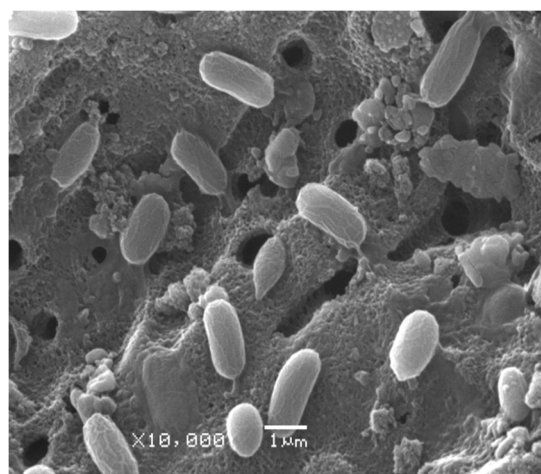
(a) *Bacillus subtilis*+ CA-A, 1:5000



(b) *Bacillus cereus* +CA-A, 1:5000



(c) *Bacillus subtilis* + CA-A, 1:10,000



(d) *Bacillus cereus* +CA-A, 1:10,000

Figure 5. SEM images of the bacteria *Bacillus subtilis* and *Bacillus cereus* adsorbed on the enterosorbent CA-A at different magnification scales.

The analysis of the images shown in Figure 5 highlights that the studied bacteria are adsorbed on the outer surface of the carbonic enterosorbent. This is explained by the fact that the length of the bacteria is within the dimensions of 1–6 μm , a size that exceeds several times the diameter of the macropores of the carbon adsorbent.

The FTIR spectra of *B. subtilis*, *B. cereus* bacteria adsorbed on the AC-A enterosorbent and the intact AC-A enterosorbent are shown in the Figure 6.

Figure 6 shows the FTIR spectra of AC-A activated carbon and adsorbent samples on which *Bacillus subtilis* and *Bacillus cereus* bacteria were immobilized. It is observed that for the samples on which the bacteria were adsorbed, there are adsorption bands different from those of activated carbon, so the band between 660–850 cm^{-1} with a maximum of 750 cm^{-1} is due to the presence of saturated primary aliphatic amides, the band included between 1057–1330 cm^{-1} with a maximum of 1190 cm^{-1} is due to the presence of the C-O bond in ketals and acetals in carbohydrates contained in bacteria. The band 2130–2330 cm^{-1} is characteristic for isocyanate groups, and the band 1950–2090 cm^{-1} is due to the presence of isothiocyanate groups [27–29]. FTIR spectra, as well as SEM photographs, indicate the presence of bacteria on the surface of AC-A activated carbon.

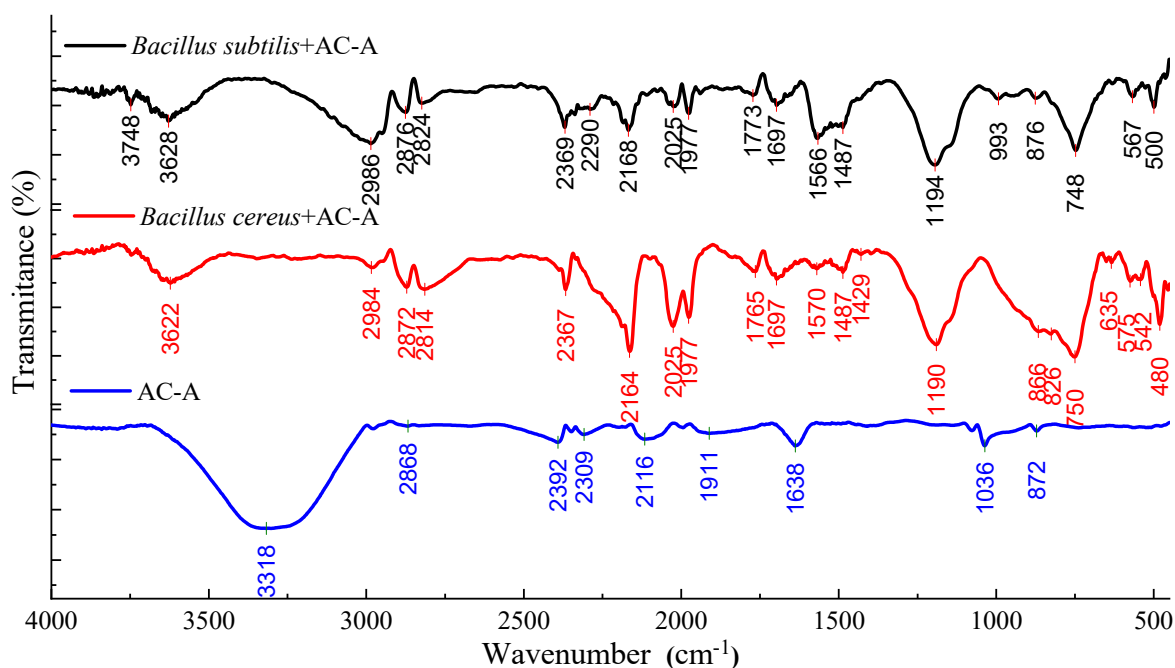


Figure 6. FTIR spectra of *B. subtilis* and *B. cereus* bacteria adsorbed on the AC-A enterosorbent and the intact AC-A enterosorbent.

4. Conclusions

1. The method of synthesis of activated carbon in a fluidized layer allows us to obtain carbon enterosorbents with quality indices that correspond to the requirements imposed by the European Pharmacopoeia Monograph.
2. Given that the size of the bacteria is much larger than the diameter of the carbon adsorbent macropores, the adsorption balance of bacteria is established relatively quickly in 75–90 min, and the immobilization of bacteria is achieved on the geometric surface of activated carbon. This phenomenon is also confirmed by the SEM studies presented in the paper.
3. The study of the dependence of adsorption processes at different temperatures highlights the fact that the process is exothermic, i.e., with increasing temperature the value of adsorption decreases. The pH value of the solution has a different influence. In the case of *Bacillus subtilis* the decrease in pH leads to an increase in the amount of immobilized bacteria per unit area of carbon adsorbent, and in the case of *Bacillus cereus* the effect is the opposite, a decrease in pH leads to a decrease in the number of immobilized bacteria on the carbonic enterosorbent.
4. The analysis of FTIR spectra highlights the fact that bacteria are immobilized through the interaction of basic groups such as amines, amides, and pyrenes from their structure with carboxylic, lactonic, and phenolic groups on the surface of activated carbons.

Author Contributions: Conceptualization, L.L. and T.L.; Data curation, L.L. and O.P.; Formal analysis, L.L., O.P. and N.T.; Funding acquisition, T.L. and O.P.; Investigation, L.L., O.P. and N.T.; Methodology, L.L., O.P., N.T. and T.L.; Supervision, T.L.; Visualization, O.P. and L.L.; Writing—original draft, L.L. and T.L.; Writing—review and editing, L.L., T.L. and O.P. All authors have read and agreed to the published version of the manuscript.

Funding: This article was written with the financial support of the Project “Reducing the impact of toxic chemicals on the environment and health by using adsorbents and catalysts obtained from local raw materials”, DISTOX, 20.80009.7007.21.

Acknowledgments: The authors are grateful to the National Collection of Non-Pathogenic Microorganisms within the Institute of Microbiology and Biotechnology of the Republic of Moldova for kindly providing bacterial strains for testing.

Conflicts of Interest: The authors declare no conflict of interest.

References

1. Fatullayeva, S.; Tagiyev, D.; Zeynalov, N. A review on enterosorbents and their application in clinical practice: Removal of toxic metals. *Colloid Interface Sci. Commun.* **2021**, *45*, 100545. [[CrossRef](#)]
2. Olson, K.R.; Anderson, I.B.; Benowitz, N.L.; Blanc, P.D.; Clark, R.F.; Kearney, T.E.; Kim-Katz, S.Y.; Wu, A.H.B. *Poisoning & Drug Overdose*, 6th ed.; Olson, K.R., Anderson, I.B., Eds.; McGraw-Hill Medical: New York, NY, USA, 2012; ISBN 978-0-07-166833-0.
3. Pimpukdee, K.; Kubena, L.F.; Bailey, C.A.; Huebner, H.J.; Afriyie-Gyawu, E.; Phillips, T.D. Aflatoxin-induced toxicity and depletion of hepatic vitamin A in young broiler chicks: Protection of chicks in the presence of low levels of NovaSil PLUS in the diet. *Poult. Sci.* **2004**, *83*, 737–744. [[CrossRef](#)] [[PubMed](#)]
4. Phillips, T.D.; Afriyie-Gyawu, E.; Williams, J.; Huebner, H.; Ankrah, N.-A.; Ofori-Adjei, D.; Jolly, P.; Johnson, N.; Taylor, J.; Marroquin-Cardona, A.; et al. Reducing human exposure to aflatoxin through the use of clay: A review. *Food Addit. Contam. Part A Chem. Anal. Control Expo. Risk Assess.* **2008**, *25*, 134–145. [[CrossRef](#)] [[PubMed](#)]
5. Rong, X.; Chen, W.; Huang, Q.; Cai, P.; Liang, W. Pseudomonas putida adhesion to goethite: Studied by equilibrium adsorption, SEM, FTIR and ITC. *Colloids Surf. B Biointerfaces* **2010**, *80*, 79–85. [[CrossRef](#)] [[PubMed](#)]
6. Cheng, X.; Zheng, J.; Lin, A.; Xia, H.; Zhang, Z.; Gao, Q.; Lv, W.; Liu, H. A review: Roles of carbohydrates in human diseases through regulation of imbalanced intestinal microbiota. *J. Funct. Foods* **2020**, *74*, 104197. [[CrossRef](#)]
7. Wei, S.; Bahl, M.I.; Baunwall, S.M.D.; Hvas, C.L.; Licht, T.R. Determining Gut Microbial Dysbiosis: A Review of Applied Indexes for Assessment of Intestinal Microbiota Imbalances. *Appl. Environ. Microbiol.* **2021**, *87*, e00395-21. [[CrossRef](#)]
8. Venkova, T.; Yeo, C.C.; Espinosa, M. Editorial: The Good, The Bad, and The Ugly: Multiple Roles of Bacteria in Human Life. *Front. Microbiol.* **2018**, *9*, 1702. [[CrossRef](#)]
9. Singhrao, S.K.; Robinson, S.; Harding, A. The Role of Bacteria in Personalized Nutrition. In *Trends in Personalized Nutrition*; Elsevier: Amsterdam, The Netherlands, 2019; pp. 81–104. ISBN 9780128164037.
10. Flint, H.J.; Scott, K.P.; Louis, P.; Duncan, S.H. The role of the gut microbiota in nutrition and health. *Nat. Rev. Gastroenterol. Hepatol.* **2012**, *9*, 577–589. [[CrossRef](#)]
11. Dekaboruah, E.; Suryavanshi, M.V.; Chettri, D.; Verma, A.K. Human microbiome: An academic update on human body site specific surveillance and its possible role. *Arch. Microbiol.* **2020**, *202*, 2147–2167. [[CrossRef](#)]
12. Maurin, M.; Raoult, D. Q fever. *Clin. Microbiol. Rev.* **1999**, *12*, 518–553. [[CrossRef](#)]
13. Crump, J.A.; Mintz, E.D. Global trends in typhoid and paratyphoid Fever. *Clin. Infect. Dis.* **2010**, *50*, 241–246. [[CrossRef](#)] [[PubMed](#)]
14. Anevlavis, S.; Bouros, D. Community acquired bacterial pneumonia. *Expert Opin. Pharmacother.* **2010**, *11*, 361–374. [[CrossRef](#)] [[PubMed](#)]
15. Kumar, V.; Abbas, A.K.; Aster, J.C.; Perkins, J.A. (Eds.) *Robbins Basic Pathology*; Elsevier: Philadelphia, PA, USA, 2018; ISBN 9780323394130.
16. Mock, M.; Fouet, A. Anthrax. *Annu. Rev. Microbiol.* **2001**, *55*, 647–671. [[CrossRef](#)]
17. Howell, C.A.; Mikhalovsky, S.V.; Markaryan, E.N.; Khovanov, A.V. Investigation of the adsorption capacity of the enterosorbent Enterogel for a range of bacterial toxins, bile acids and pharmaceutical drugs. *Sci. Rep.* **2019**, *9*, 5629. [[CrossRef](#)] [[PubMed](#)]
18. Hong, Z.; Rong, X.; Cai, P.; Liang, W.; Huang, Q. Effects of Temperature, pH and Salt Concentrations on the Adsorption of Bacillus subtilis on Soil Clay Minerals Investigated by Microcalorimetry. *Geomicrobiol. J.* **2011**, *28*, 686–691. [[CrossRef](#)]
19. Zemnukhova, L.; Kharchenko, U.; Beleneva, I. Biomass derived silica containing products for removal of microorganisms from water. *Int. J. Environ. Sci. Technol.* **2015**, *12*, 1495–1502. [[CrossRef](#)]
20. Knezev, A. *Microbial Activity in Granular Activated Carbon Filters in Drinking Water Treatment*; Wageningen University: Wageningen, The Netherlands, 2015; ISBN 9789462572447.
21. Rivera-Utrilla, J.; Bautista-Toledo, I.; Ferro-García, M.A.; Moreno-Castilla, C. Activated carbon surface modifications by adsorption of bacteria and their effect on aqueous lead adsorption. *J. Chem. Technol. Biotechnol.* **2001**, *76*, 1209–1215. [[CrossRef](#)]
22. Burchacka, E.; Pstrowska, K.; Beran, E.; Fałtynowicz, H.; Chojnacka, K.; Kułczyński, M. Antibacterial Agents Adsorbed on Active Carbon: A New Approach for S. aureus and E. coli Pathogen Elimination. *Pathogens* **2021**, *10*, 1066. [[CrossRef](#)]
23. Maksimova, Y.G. Microorganisms and Carbon Nanotubes: Interaction and Applications (Review). *Appl. Biochem. Microbiol.* **2019**, *55*, 1–12. [[CrossRef](#)]
24. Wu, P.; Wang, Z.; Bhatnagar, A.; Jeyakumar, P.; Wang, H.; Wang, Y.; Li, X. Microorganisms-carbonaceous materials immobilized complexes: Synthesis, adaptability and environmental applications. *J. Hazard. Mater.* **2021**, *416*, 125915. [[CrossRef](#)]
25. Chwastowski, J.; Staroń, P. Influence of Saccharomyces cerevisiae yeast cells immobilized on Cocos nucifera fibers for the adsorption of Pb(II) ions. *Colloids Surf. A: Physicochem. Eng. Asp.* **2022**, *632*, 127735. [[CrossRef](#)]
26. *European Pharmacopoeia*, 10th ed.; Council of Europe, European Directorate for the Quality of Medicines and Healthcare: Strasbourg, France, 2019; ISBN 978-92-871-8912-7.

-
27. Kuptsov, A.H.; Zhizhin, G.N. (Eds.) *Handbook of Fourier Transform Raman and Infrared Spectra of Polymers*; Elsevier: Amsterdam, The Netherlands; New York, NY, USA, 1998; ISBN 0-444-82620-3.
 28. Larkin, P. (Ed.) *Infrared and Raman Spectroscopy: Principles and Spectral Interpretation*; Elsevier: Amsterdam, The Netherlands; Boston, MA, USA, 2011; ISBN 978-0-12-386984-5.
 29. Stuart, B.H. (Ed.) *Infrared Spectroscopy: Fundamentals and Applications*; Wiley & Sons: Chichester, UK; Hoboken, NJ, USA, 2005; ISBN 9780470011140.